The Frequency Domain

1   Overview

In these notes we describe a fundamental tool in signal processing: frequency representations. Section 2 introduces the Fourier series, which is a frequency representation for continuous functions defined on an interval. Section 3 is dedicated to the celebrated sampling theorem, which is a pillar of modern signal processing. Section 4 describes the discrete Fourier transform, which is the discrete counterpart of the Fourier series. Section 5, 6 and 7 discuss the Fourier series, the sampling theorem and the discrete Fourier transform in multiple dimensions.

2   The Fourier series

Structured objects such as images, audio sequences, and videos are often modeled as functions of time or space known as signals. In order to analyze and process signals, it is useful to represent them as linear combinations of simpler functions. Let us consider the vector space of complex-valued square-integrable functions defined on an interval $[a, b] \subset \mathbb{R}$ with the standard inner product,

$$\langle x, y \rangle := \int_a^b x(t) \, \overline{y(t)} \, \mathrm{d}t. \tag{1}$$

To express a function $x : [a, b] \to \mathbb{R}$ in terms of an orthonormal basis of functions $g_1, g_2 \dots$, each defined from $[a, b]$ to $\mathbb{R}$ all we need to do is compute the coefficients

$$c[j] := \langle x, g_j \rangle. \tag{2}$$

Indeed, by the properties of orthonormal bases,

$$x = \sum_j c[j] g_j. \tag{3}$$

Signals often have periodic structure due to repeating patterns. In this section, we describe a representation that decomposes a signal into periodic components that oscillate at different *frequencies*. This often uncovers structure that is difficult to interpret or manipulate otherwise.

The frequency of a periodic signal is the inverse of its period. By far the most popular basis functions with fixed frequencies are sinusoids. Sinusoids are smooth oscillating functions of the form

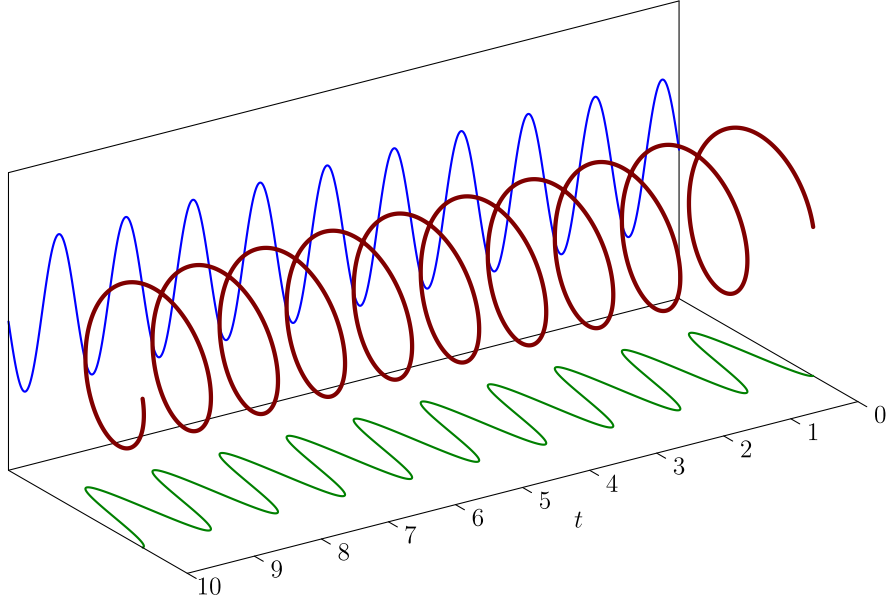$$a \cos(2\pi f t + \theta), \tag{4}$$

Figure 1: Complex sinusoid (dark red) as a function of time. The real part (green) is a cosine function. The imaginary part (blue) is a sine function.

where $a \in \mathbb{R}$ is the amplitude, $f \in \mathbb{R}$ the frequency, t is the time index, and $\theta \in [0, 2\pi]$ is the phase. A sinusoid with frequency f is periodic with period $T := 1/f$. Expressing a signal in terms of the cosine (or sine) function as in Eq. (4) is not very convenient. The function depends nonlinearly on the phase θ, so there are infinite possible basis functions associated to each frequency. An elegant solution is to use complex-valued sinusoids instead.

Definition 2.1 (Complex sinusoid). *The complex sinusoid with frequency $f \in R$ is given by*

$$\exp(i2\pi ft) := \cos(2\pi ft) + i\sin(2\pi ft). \tag{5}$$

Figure 1 shows a complex sinusoid, along with its real and imaginary parts. Note that complex sinusoids can have negative frequencies. This just changes their imaginary component to $-\sin(2\pi ft)$, instead of $\sin(2\pi ft)$. Any real sinusoid with frequency f can be represented as the sum of two complex sinusoids with frequencies f and $-f$ respectively:

$$\cos(2\pi ft + \theta) = \frac{\exp(i2\pi ft + i\theta) + \exp(-i2\pi ft - i\theta)}{2} \tag{6}$$

$$= \frac{\exp(i\theta)}{2}\exp(i2\pi ft) + \frac{\exp(-i\theta)}{2}\exp(-i2\pi ft). \tag{7}$$

Crucially, the phase is now encoded in the complex amplitude of the sinusoid. As a result, from a linear-algebra perspective, the subspace spanned by the two complex sinusoids with frequencies f and $-f$ contains all possible real sinusoids with frequency f. In particular, if we add two sinusoids with the same frequency, but different amplitudes and phases, the result is a sinusoid with that frequency. It therefore makes sense to interpret sinusoids as basis functions, each representing a particular frequency.

2

If we are interested in obtaining a representation for functions restricted to an interval, working with orthogonal basis functions makes life much easier. The following lemma shows that for any fixed positive $T \in \mathbb{R}$, complex sinusoids with frequency equal to k/T– where k is an integer– are all orthogonal.

Lemma 2.2 (Orthogonality of complex sinusoids). *The family of complex sinusoids with integer frequencies*

$$\phi_k(t) := \exp\left(\frac{i2\pi kt}{T}\right), \qquad k \in \mathbb{Z}, \tag{8}$$

is an orthogonal set of functions on any interval of the form $[a, a+T]$, where $a, T \in \mathbb{R}$ and $T > 0$.

Proof. We have

$$\langle \phi_k, \phi_j \rangle = \int_a^{a+T} \phi_k(t) \overline{\phi_j(t)} \, dt \tag{9}$$

$$= \int_a^{a+T} \exp\left(\frac{i2\pi(k-j)t}{T}\right) dt \tag{10}$$

$$= \frac{T}{i2\pi(k-j)} \left(\exp\left(\frac{i2\pi(k-j)(a+T)}{T}\right) - \exp\left(\frac{i2\pi(k-j)a}{T}\right)\right) \tag{11}$$

$$= 0 \tag{12}$$

as long as $j \neq k$. $\qquad\square$

In words, this family includes all complex sinusoids with positive and negative frequencies whose period is an integer fraction of the length of the interval. The Fourier series is a decomposition of signals as a sum of these basis functions.

Definition 2.3 (Fourier series). *The Fourier series coefficients of a function $x \in \mathcal{L}_2[a, a+T]$, $a, T \in \mathbb{R}$, $T > 0$, are given by*

$$\hat{x}[k] := \langle x, \phi_k \rangle = \int_a^{a+T} x(t) \exp\left(-\frac{i2\pi kt}{T}\right) dt. \tag{13}$$

The Fourier series of order k_c is defined as

$$\mathcal{F}_{k_c}\{x\} := \frac{1}{T} \sum_{k=-k_c}^{k_c} \hat{x}[k]\phi_k. \tag{14}$$

The Fourier series of a signal x is defined as $\lim_{k_c \to \infty} \mathcal{F}_{k_c}\{x\}$.

The basis functions have norm $\sqrt{T}$. We can interpret the Fourier series of order k_c as a projection of the function onto the span of the complex sinusoids with frequencies up to k_c/T. By Lemma 2.2 the sinusoids scaled by $1/\sqrt{T}$ are orthonormal so

$$\mathcal{P}_{\text{span}(\{\phi_{-k_c}, \phi_{-k_c+1}, \dots, \phi_{k_c}\})} \, x = \sum_{k=-k_c}^{k_c} \left\langle x, \frac{1}{\sqrt{T}}\phi_k \right\rangle \frac{1}{\sqrt{T}}\phi_k \tag{15}$$
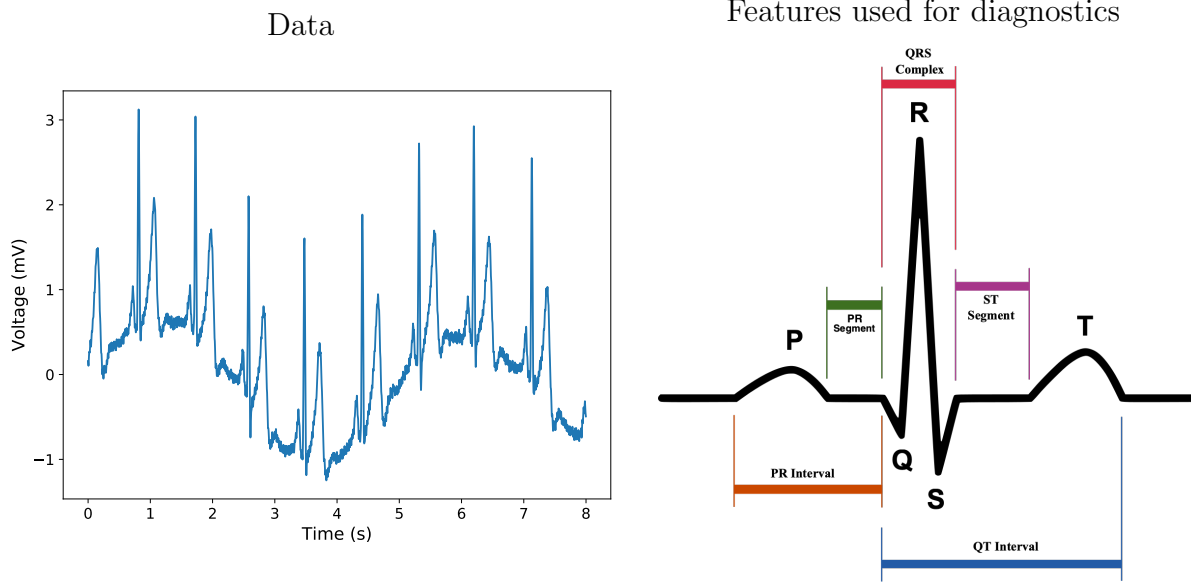
$$= \mathcal{F}_{k_c}\{x\}. \tag{16}$$

Figure 2: The left image shows an electrocardiogram (ECG) with a duration of 8 s. The top right image shows the features that are relevant for medical diagnostics in a typical ECG.

Figure 3 shows the Fourier series coefficients of the electrocardiogram signal in Figure 2. Figure 4 shows the kth-order partial Fourier series of the signal for different values of k_c, together with the corresponding real sinusoidal components obtained by combining $\hat{x}_{k_c}\phi_{k_c}$ and $\hat{x}_{-k_c}\phi_{-k_c}$. As k_c increases, the approximation improves. Remarkably, if the function is integrable, the approximation eventually converges to the function. We omit the proof of this result, which is beyond the scope of these notes.

Theorem 2.4 (Convergence of Fourier series). *For any function $x \in \mathcal{L}_2[0, T)$, where $a, T \in \mathbb{R}$ and $T > 0$,*

$$\lim_{k \to \infty} ||x - \mathcal{F}_k\{x\}||_{\mathcal{L}_2} = 0. \tag{17}$$

By Theorem 2.4 we can represent any square-integrable function defined on an interval by using its Fourier coefficients, which are often known as the *spectrum* of the function. It is worth noting that one can generalize this representation to functions defined on the whole real line by considering real-valued frequencies, which yields the Fourier transform.

Example 2.5 (Filtering an electrocardiogram). Electrocardiography is a method to record heart activity by using electrodes to measure electrical changes on the skin. Figure 2 also shows the standard features used by doctors to perform diagnostics using ECGs[1]. Unfortunately, the data contains other periodic patterns that make it difficult to visualize these features. Decomposing the signal in components with different frequencies is very useful to remove such perturbations. The low-frequency components of the ECG signal in Figure 2 produce significant *baseline wandering*, which are slowly-varying fluctuations typically caused by motion of the recording apparatus or the patient, or by breathing. In addition, the Fourier series coefficients of the data, shown in Figure 3 reveal a strong component at 50 Hz. This is caused by interference from the electric grid,

---

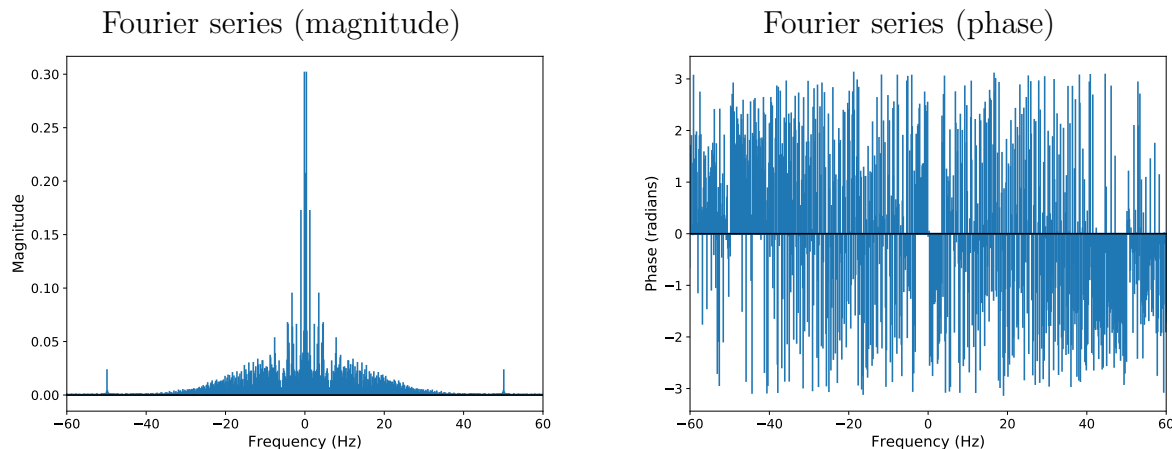[1]The image is borrowed from https://commons.wikimedia.org/wiki/File:SinusRhythmLabels.svg

Figure 3: Magnitude (left) and phase (right) of the Fourier coefficients of the ECG data in the left image of Figure 2.

which transmits electricity exactly at that frequency. In order to use the electrocardiogram for diagnostics, we would like to eliminate these effects, since they are not associated to heart activity. We can be achieve this by removing the corresponding Fourier components from the Fourier series representation, an approach known as *filtering* in the signal processing literature. Removing the low-frequency components gets rid of baseline wandering. Removing the component at 50 Hz removes the electric-grid interference. Figure 5 shows that the approach succeeds in highlighting the features related to heart activity. △

3 Sampling bandlimited functions

Signals often model continuous objects, such as sound, or images, which need to be measured in order to be stored and processed. A natural way to measure signals is to *sample* them, which means recording their value at certain fixed locations. In this section, we consider the problem of sampling continuous signals that consist of a finite number of sinusoidal components. Under certain conditions it is possible to reconstruct such signals exactly from the samples. At a first glance, this may sound counterintuitive because the functions are continuous. However, they also have a finite parametrization in terms of their Fourier coefficients, and this parametrization can be recovered from a finite number of samples.

We begin by considering a single complex sinusoid ϕ_k with frequency k/T defined on an interval of length T, which we assume to be $[0, T)$ without loss of generality. The sinusoid is sampled on a uniform grid with N equispaced points that divide an interval of length T into N segments of length T/N: $\phi_k \left(\frac{0}{N} \right)$, $\phi_k \left(\frac{T}{N} \right)$, $\phi_k \left(\frac{2T}{N} \right)$, ..., $\phi_k \left(\frac{(N-1)T}{N} \right)$. We immediately encounter a problem: these samples are exactly the same as if the frequency of the sinusoid were instead $\frac{k+pN}{T}$ for any
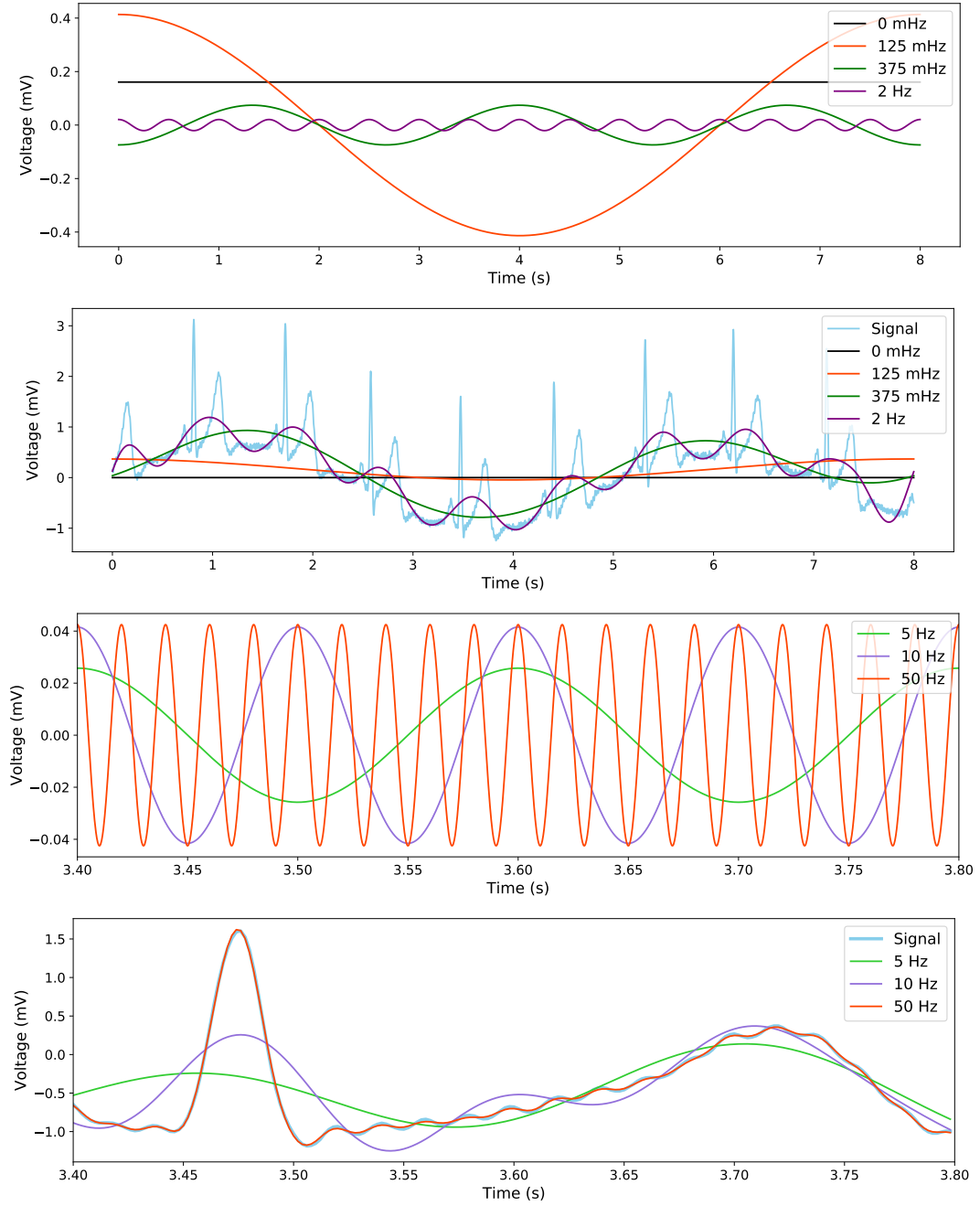
Figure 4: The top image shows components of the Fourier series of the ECG signal from Figure 2. The third image shows zoomed components corresponding to higher frequencies. The second and fourth image show the Fourier series of the signal truncated at different frequencies.
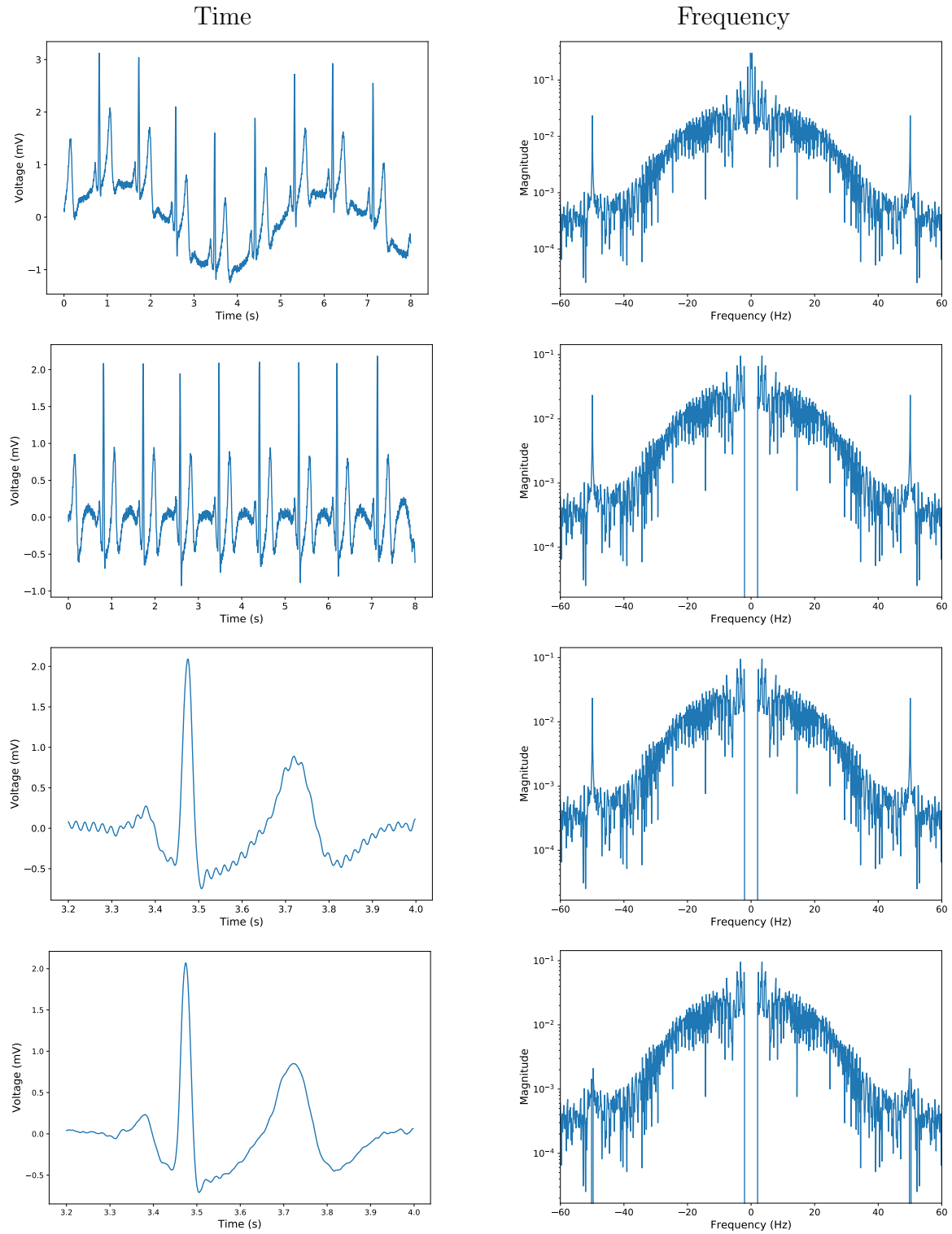
6

Figure 5: The ECG data from Example 2.5 (top row) is filtered to first remove low-frequency components (second and third rows) and then electric-grid interference at 50 Hz (bottom row). The left column displays the signals in the time domain. The right columns shows the magnitude of the corresponding Fourier series coefficients.
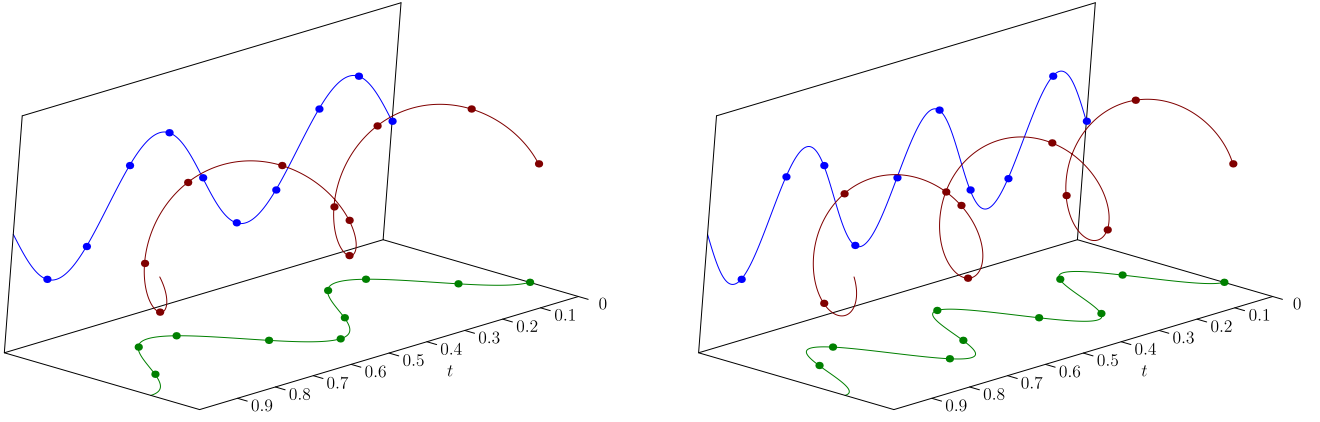
Figure 6: Discrete complex sinusoids ψ_2 (left) and ψ_3 (right) for $N = 10$, displayed in red. The real and imaginary parts are shown in green and blue respectively.

integer p:

$$\phi_k\left(\frac{j}{N}\right) = \exp\left(\frac{i2\pi kj}{NT}\right) \tag{18}$$

$$= \exp\left(\frac{i2\pi(k+pN)j}{NT}\right) \tag{19}$$

$$= \phi_{k+pN}\left(\frac{j}{N}\right). \tag{20}$$

It is impossible to distinguish complex sinusoids with frequencies $\frac{k+pN}{T}$ from these samples. However, frequencies that are restricted to a fixed interval of length N are distinguishable. To simplify the exposition, let $N := 2k_c + 1$ for some positive integer k_c. Then if $|k| \leq k_c$, there is no value of $p \neq 0$ such that $k + pN$ is between $-k_c$ and k_c, i.e. the frequencies in that interval are distinguishable from the samples. The vector of samples corresponding to each of these frequencies can be interpreted as a discrete sinusoid.

Definition 3.1 (Discrete complex sinusoids). *The discrete complex sinusoid $\psi_k \in \mathbb{C}^N$ with integer frequency k is defined as*

$$\psi_k[j] := \exp\left(\frac{i2\pi kj}{N}\right), \qquad 0 \leq j, k \leq N - 1. \tag{21}$$

Figure 6 shows ψ_2 and ψ_3 for $N := 10$.

Discrete complex sinusoids form an orthonormal basis of $\mathbb{C}^N$ if we scale them by $1/\sqrt{N}$.

Lemma 3.2 (Orthonormal sinusoidal basis). *The discrete complex exponentials $\frac{1}{\sqrt{N}}\psi_0$, ..., $\frac{1}{\sqrt{N}}\psi_{N-1}$ form an orthonormal basis of $\mathbb{C}^N$.*

8

Proof. Each vector has ℓ_2 norm equal to $\sqrt{N}$,

$$||\psi_k||_2^2 = \sum_{j=0}^{N-1} |\psi_k[j]|^2 \tag{22}$$

$$= \sum_{j=0}^{N-1} 1 \tag{23}$$

$$= N, \tag{24}$$

and

$$\langle \psi_k, \psi_l \rangle = \sum_{j=0}^{N-1} \psi_k[j] \overline{\psi_l[j]} \tag{25}$$

$$= \sum_{j=0}^{N-1} \exp\left(\frac{i2\pi(k-l)j}{N} \right) \tag{26}$$

$$= \frac{1 - \exp\left(\frac{i2\pi(k-l)N}{N} \right)}{1 - \exp\left(\frac{i2\pi(k-l)}{N} \right)} \tag{27}$$

$$= 0, \tag{28}$$

if $k \neq l$. Since there are N vectors in the set and they are linearly independent, they form a basis of $\mathbb{C}^N$. $\qquad \square$

This result means that if a signal can be represented as a linear combination of continuous sinusoids with frequencies between $-k_c$ and k_c then its coefficients can be retrieved exactly from $N := 2k_c + 1$ samples. Such signals are called bandlimited signals. Signals with this property are said to be bandlimited.

Definition 3.3 (Bandlimited signal). *A signal is bandlimited with a cut-off frequency k_c if it is equal to its Fourier series representation of order k_c, i.e.*

$$x(t) = \sum_{k=-k_c}^{k_c} \hat{x}[k] \exp\left(\frac{i2\pi kt}{T} \right). \tag{29}$$

Assume we measure a bandimited signal x with cut-off frequency k_c to obtain the samples: $x\left(\frac{0}{N}\right)$, $x\left(\frac{T}{N}\right)$, $x\left(\frac{2T}{N}\right)$, ..., $x\left(\frac{(N-1)T}{N}\right)$. The Fourier series of the bandlimited signal provides a linear equation relating the samples and the Fourier coefficients of the signal:

$$x\left(\frac{jT}{N}\right) = \sum_{k=-k_c}^{k_c} \hat{x}_k \exp\left(\frac{i2\pi kjT}{NT} \right) \tag{30}$$

$$= \sum_{k=-k_c}^{k_c} \hat{x}_k \exp\left(\frac{i2\pi kj}{N} \right). \tag{31}$$

This yields the following system of linear equations:

$$
\begin{bmatrix}
x\left(\frac{0}{N}\right) \\
x\left(\frac{T}{N}\right) \\
\cdots \\
x\left(\frac{jT}{N}\right) \\
\cdots \\
x\left(T - \frac{T}{N}\right)
\end{bmatrix}
=
\begin{bmatrix}
1 & 1 & \cdots & 1 \\
\exp\left(\frac{i2\pi(-k_c)}{N}\right) & \exp\left(\frac{i2\pi(-k_c+1)}{N}\right) & \cdots & \exp\left(\frac{i2\pi k_c}{N}\right) \\
\cdots & \cdots & \cdots & \cdots \\
\exp\left(\frac{i2\pi(-k_c)j}{N}\right) & \exp\left(\frac{i2\pi(-k_c+1)j}{N}\right) & \cdots & \exp\left(\frac{i2\pi k_c j}{N}\right) \\
\cdots & \cdots & \cdots & \cdots \\
\exp\left(\frac{i2\pi(-k_c)(N-1)}{N}\right) & \exp\left(\frac{i2\pi(-k_c+1)(N-1)}{N}\right) & \cdots & \exp\left(\frac{i2\pi k_c(N-1)}{N}\right)
\end{bmatrix}
\begin{bmatrix}
\hat{x}[-k_c] \\
\hat{x}[-k_c+1] \\
\cdots \\
\hat{x}[k_c]
\end{bmatrix}
$$

More succinctly, we have

$$
x_{[N]} = \widetilde{F}_{[N]}\hat{x}_{[k_c]}, \tag{32}
$$

where $x_{[N]}$ is the vector of samples and $\hat{x}_{[k_c]}$ is the vector of Fourier coefficients. If the matrix $\widetilde{F}_{[N]}$ is invertible, we can recover the Fourier coefficients from the samples and completely recover the bandlimited function. This is the case as long as $N \geq 2k_c + 1$.

Theorem 3.4 (Nyquist-Shannon-Kotelnikov sampling theorem). *Any bandlimited signal $x \in \mathcal{L}_2[0,T]$, where $T > 0$, with cut-off frequency k_c can be recovered exactly from N uniformly spaced samples $x(0)$, $x(T/N)$, ..., $x(T - T/N)$ as long as*

$$
N \geq 2k_c + 1, \tag{33}
$$

where $2k_c + 1$ is known as the Nyquist rate. *The Fourier series coefficients $\hat{x}_{[k_c]}$ can be recovered from the vector of samples $x_{[N]}$ as follows*

$$
\hat{x}_{[k_c]} = \frac{1}{N}\widetilde{F}_{[N]}^* x_{[N]}, \tag{34}
$$

where $\widetilde{F}_{[N]}$ is defined in Eq. (32).

Proof. Note that for $-k_c \leq k \leq -1$ and $0 \leq j \leq N - 1$,

$$
\exp\left(\frac{i2\pi kj}{N}\right) = \exp\left(\frac{i2\pi(N+k)j}{N}\right), \tag{35}
$$

so the columns of matrix $\widetilde{F}_{[N]}$ in Eq. (32) equal $\psi_{N-k_c}, \ldots, \psi_{N-1}, \psi_0, \ldots, \psi_{k_c}$. If $N \geq 2k_c + 1$, then no column is repeated. In that case, by Lemma 7.2 the matrix $\widetilde{F}_{[N]}$ has orthogonal columns with norm $\sqrt{N}$, which implies

$$
\frac{1}{N}\widetilde{F}_{[N]}^*\widetilde{F}_{[N]} = \left(\frac{1}{\sqrt{N}}\widetilde{F}_{[N]}\right)^* \frac{1}{\sqrt{N}}\widetilde{F}_{[N]} = I. \tag{36}
$$

$\square$

The sampling theorem is very useful in audio processing. It turns out that the range of frequencies that human beings can hear is from 20 Hz to 20 kHz. The sampling theorem therefore dictates that audio should be sampled at a rate of at least 40 kHz. Typical rates used in practice are 44.1 kHz (CD), 48 kHz, 88.2 kHz, or 96 kHz.

In practice, signals are never exactly bandlimited. It is therefore very important to understand what happens if we sample a signal that is not bandlimited and try to reconstruct it under the assumption that it is. In general, from N samples, we can only hope to estimate the first $2k_c + 1$ Fourier coefficients, where k_c is such that $N := 2k_c + 1$. The following lemma establishes that, unless the signal is exactly bandlimited with cut-off frequency k_c, the estimated Fourier coefficients are *not* equal to the true coefficients because there is additive interference from coefficients corresponding to higher frequencies. This phenomenon is known as *aliasing*.

Lemma 3.5 (Aliasing). *Let x be a defined on $[0, T)$, $T > 0$, and let $x_{[N]}$ be a vector of N samples of x at 0, T/N, $2T/N$, ...$T - T/N$. The vector*

$$\hat{x}^{\text{rec}}[k] := \frac{1}{N}(\widetilde{F}^*_{[N]} x_{[N]})[k], \quad -k_{\text{samp}} \leq k \leq k_{\text{samp}}, \tag{37}$$

denotes the estimate of the kth Fourier coefficient of x computed under the assumption that the signal is bandlimited with a cut-off frequency of k_{samp}, where $N = 2k_{\text{samp}} + 1$. We have

$$\hat{x}^{\text{rec}}[k] = \sum_{\{(m-k) \bmod N = 0\}} \hat{x}[m], \tag{38}$$

where $\hat{x}$ denotes the true Fourier coefficients of x.

Proof. We denote the true cut-off frequency of x, which can be arbitrarily large by k_{true} (the argument can be extended to non-bandlimited funcions). By the definition of $\widetilde{F}_{[N]}$

$$\hat{x}^{\text{rec}}[k] = \frac{1}{N}(\widetilde{F}^*_{[N]} x_{[N]})[k] \tag{39}$$

$$= \frac{1}{N} \sum_{j=0}^{N-1} \exp\left(-\frac{i2\pi kj}{N}\right) \sum_{m=-k_{\text{true}}}^{k_{\text{true}}} \hat{x}[m] \exp\left(\frac{i2\pi mj}{N}\right) \tag{40}$$

$$= \frac{1}{N} \left\langle \psi_k, \sum_{(m-k) \bmod N = 0} \hat{x}[m] \psi_k \right\rangle \tag{41}$$

$$= \sum_{\{(m-k) \bmod N = 0\}} \hat{x}[m]. \tag{42}$$

$\square$

The reason for aliasing is that samples from a sinusoid with frequency m are identical to the samples from a sinusoid with frequency $k = m \bmod N$, where N is the number of samples. This is illustrated in the following example and Figure 7. The sampling theorem establishes that if the only sinusoidal components present in a signal all have frequencies less than the Nyquist rate, then there is no possible confusion.
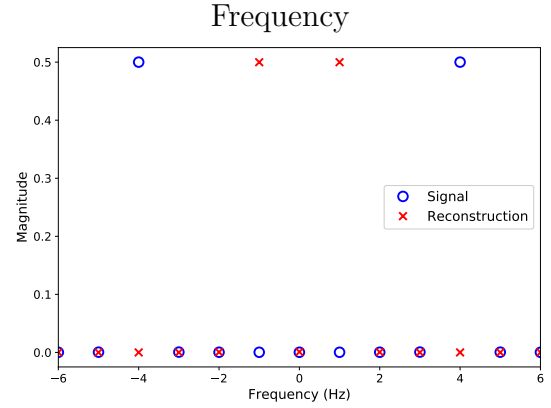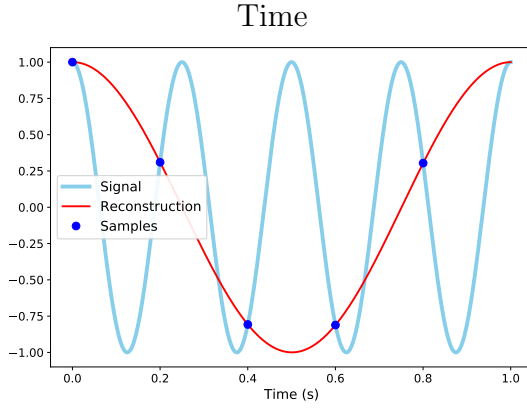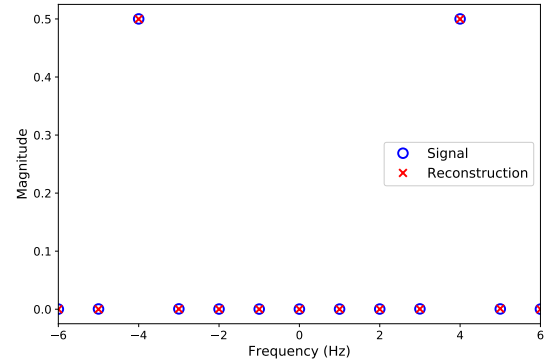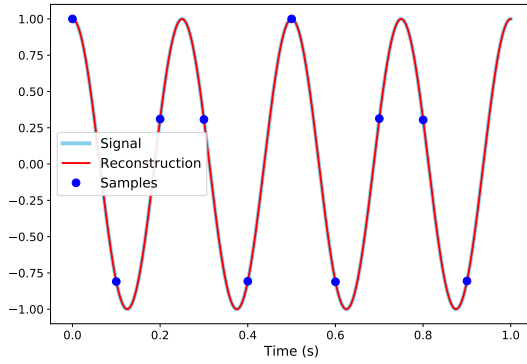
Figure 7: Illustration of aliasing (top row) and perfect recovery (bottom row) of a real sinusoid from equispaced samples, as described in Example 3.6. The left column shows the samples, the original signal and the recovered signal in the time domain. The right column shows the corresponding Fourier coefficients.

12

Example 3.6 (Sampling a real sinusoid). Let us consider a real sinusoid with frequency equal to 4 Hz

$$x(t) := \cos(8\pi t) \tag{43}$$
$$= 0.5\exp(-i2\pi 4 t) + 0.5\exp(i2\pi 4 t) \tag{44}$$

measured over one second, i.e. $T = 1$ s. The Fourier coefficients of the original signal are all zero except for $\hat{x}[-4] = 0.5$ and $\hat{x}[4] = 0.5$, so the signal is bandlimited with cut-off frequency $k_c := 4$. If the number of samples N is larger than $2k_c + 1 = 9$ then by Theorem 6.2 the Fourier coefficients, and hence the signal, can be reconstructed perfectly, as shown in Figure 7 for $N = 10$.

To illustrate what happens if $N < 2k_c + 1$ let us assume $N = 5$. In that case we can only hope to recover 5 Fourier coefficients: $k \in \{-2, -1, 0, 1, 2\}$. Applying Lemma 3.5, the Fourier coefficients corresponding to $k \in \{-2, 0, 2\}$ will be estimated to equal zero because $(4 - k) \bmod 5 \neq 0$ and $(-4 - k) \bmod 5 \neq 0$ for $k = -2, 0, 2$. For $k = -1$ we have $(4 - (-1)) \bmod N = 0$ so the corresponding estimated coefficient $\hat{x}^{\text{rec}}[-1]$ equals $\hat{x}_4 = 0.5$. Similarly, $(-4 - 1) \bmod N = 0$ so $\hat{x}^{\text{rec}}[1]$ equals $\hat{x}[-4] = 0.5$. The samples are consistent with a real sinusoid with cut-off frequency 1 Hz, as shown in Figure 7. △

Example 3.7 (Sampling an electrocardiogram). The ECG signal from Example 2.5 is only approximately bandlimited. Its approximate cut-off frequency is roughly above 50 Hz, where there is a significant contribution from electric-grid interference. In this example, we have $T = 8$ s, so 50 Hz corresponds to $k_c = 50/(1/T) = 400$. By Theorem 6.2 the number of samples should be at least 801 to avoid significant aliasing. Figure 8 shows that for $N = 1{,}000$ the aliasing is indeed almost imperceptible. In contrast, if $N = 625$ the aliasing is evident in both the time and the frequency domain. In particular the frequency component at $k = 400$ (corresponding to the electric-grid interference at 50 Hz) shows up at $k = \pm 225$, which corresponds to 28.125 Hz. This follows from Lemma 3.5 because $(400 - (-225)) \bmod 625 = 0$ and $(-400 - 225) \bmod 625 = 0$. △

4 The discrete Fourier transform

The discrete Fourier transform is a change of basis that expresses a finite-dimensional vector in terms of discrete complex sinusoids. It is the discrete counterpart of the Fourier series.

Definition 4.1 (Discrete Fourier transform). *The discrete Fourier transform (DFT) of a vector $x \in \mathbb{C}^N$ is given by*
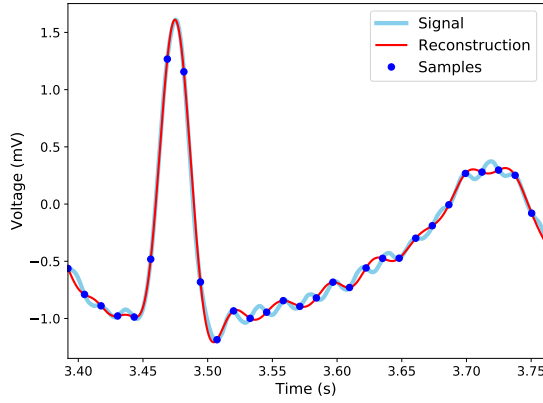
$$\hat{x} := \begin{bmatrix} 1 & 1 & 1 & \cdots & 1 \\ 1 & \exp\left(-\frac{i2\pi}{N}\right) & \exp\left(-\frac{i2\pi 2}{N}\right) & \cdots & \exp\left(-\frac{i2\pi(N-1)}{N}\right) \\ 1 & \exp\left(-\frac{i2\pi 2}{N}\right) & \exp\left(-\frac{i2\pi 4}{N}\right) & \cdots & \exp\left(-\frac{i2\pi 2(N-1)}{N}\right) \\ \cdots & \cdots & \cdots & \cdots & \cdots \\ 1 & \exp\left(-\frac{i2\pi(N-1)}{N}\right) & \exp\left(-\frac{i2\pi 2(N-1)}{N}\right) & \cdots & \exp\left(-\frac{i2\pi(N-1)^2}{N}\right) \end{bmatrix} x = F_{[N]}x. \tag{45}$$

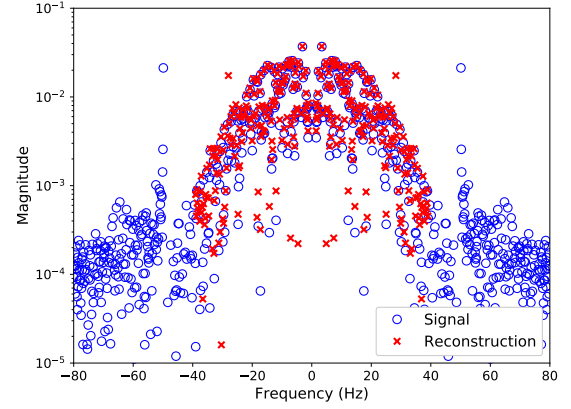*In terms of the discrete complex sinusoids in Definition 3.1,*

$$\hat{x}[k] = \langle x, \psi_k \rangle, \qquad 0 \leq k \leq N - 1. \tag{46}$$
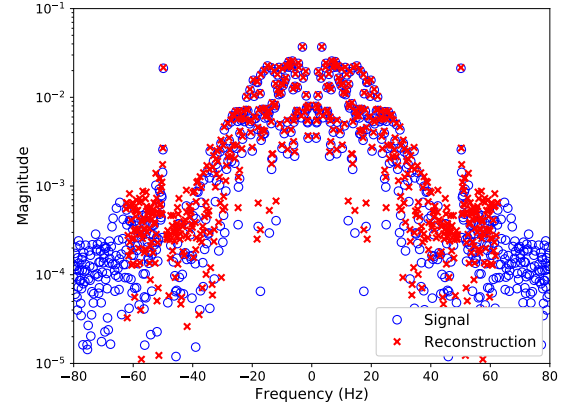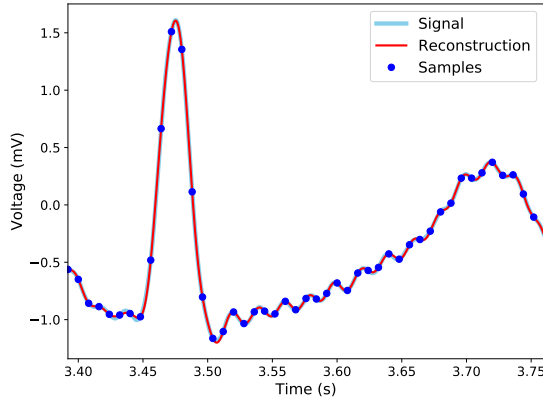
Figure 8: Effect of different sampling rates on the recovery of the ECG data from Example 2.5. The left column shows the samples, the original signal and the recovered signal in the time domain. The right column shows the corresponding Fourier coefficients. As explained in Example 3.7, if the sampling rate is not sufficiently high, there is significant aliasing (top row). This can be mitigated by increasing the rate (bottom row).

The inverse DFT of a vector $\hat{y} \in \mathbb{C}^N$ equals

$$y = \frac{1}{N} F_{[N]}^* \hat{y}. \tag{47}$$

The rows of the DFT matrix $F_{[N]}$ are exactly the same as the rows of the matrix $\widetilde{F}_{[N]}^*$ in Eq. (32), only in a different order (since for any k and any integer l $\phi_k = \phi_{k+lN}$). This observation combined with Theorem 6.2 provides an interesting interpretation of the DFT: if $x \in \mathbb{C}^N$ contains equispaced samples from a bandlimited signal x_c with cut-off frequency k_c– where $N \geq 2k_c + 1$– then the DFT of x contains the nonzero Fourier series coefficients of x_c. In addition, by Lemma 7.2 the rows (and columns) of $F_{[N]}$ are orthogonal and have norm $\sqrt{N}$, which justifies the definition of the inverse DFT.

Corollary 4.2. *The inverse DFT inverts the DFT.*

In general, the time complexity of multiplying an $N \times N$ matrix with an N-dimensional vector is N^2. However one can compute the DFT much faster. The fast-Fourier transform (FFT) algorithm exploits the structure of the DFT matrix to compute the DFT with complexity $\mathcal{O}(N \log N)$. It is difficult to overstate the importance of the FFT. Gilbert Strang has described it as *the most important numerical algorithm of our lifetime.* The main insight underlying the FFT is that the N-order DFT matrix can be expressed in terms of $N/2$-order DFT submatrices. To simplify the exposition we assume that N is even, but similar decompositions are possible for odd N.

Lemma 4.3. *Let $F_{[N]}$ denote the $N \times N$ DFT matrix, where N is even. Then for $k = 0, 1, \ldots, N/2-1$, and any vector $x \in \mathbb{C}^N$*

$$F_{[N]}x[k] = F_{[N/2]}x_{\text{even}}[k] + \exp\left(-\frac{i2\pi k}{N}\right) F_{[N/2]}x_{\text{odd}}[k], \tag{48}$$

$$F_{[N]}x[k + N/2] = F_{[N/2]}x_{\text{even}}[k] - \exp\left(-\frac{i2\pi k}{N}\right) F_{[N/2]}x_{\text{odd}}[k], \tag{49}$$

where x_{even} and x_{odd} contain the even and odd entries of x respectively.

Proof. The proof is illustrated in Figure 9. □

The Cooley-Tukey FFT algorithm exploits Lemma 4.3 to compute the DFT recursively.

Algorithm 4.4 (Cooley-Tukey Fast Fourier transform). *If $N = 1$, output $F_{[1]}x := x$. Otherwise apply the following steps:*

1. *Compute $F_{[N/2]}x_{\text{even}}$.*

2. *Compute $F_{[N/2]}x_{\text{odd}}$.*

3. *For $k = 0, 1, \ldots, N/2 - 1$ set*

$$F_{[N]}x[k] := F_{[N/2]}x_{\text{even}}[k] + \exp\left(-\frac{i2\pi k}{N}\right) F_{[N/2]}x_{\text{odd}}[k], \tag{50}$$

$$F_{[N]}x[k + N/2] := F_{[N/2]}x_{\text{even}}[k] - \exp\left(-\frac{i2\pi k}{N}\right) F_{[N/2]}x_{\text{odd}}[k]. \tag{51}$$

(a) Separation in even/odd columns and top/bottom rows.

(b) Even columns can be scaled to yield odd columns.

(c) Top even submatrix and bottom even submatrix are both an $N/2$-order DFT matrix.

(d) Application of N-order DFT matrix to an N-dimensional vector expressed in terms of two $N/2$-order DFT matrices applied to two $N/2$-dimensional vectors.

Figure 9: Illustration of the proof of Lemma 4.3 for $N := 8$.
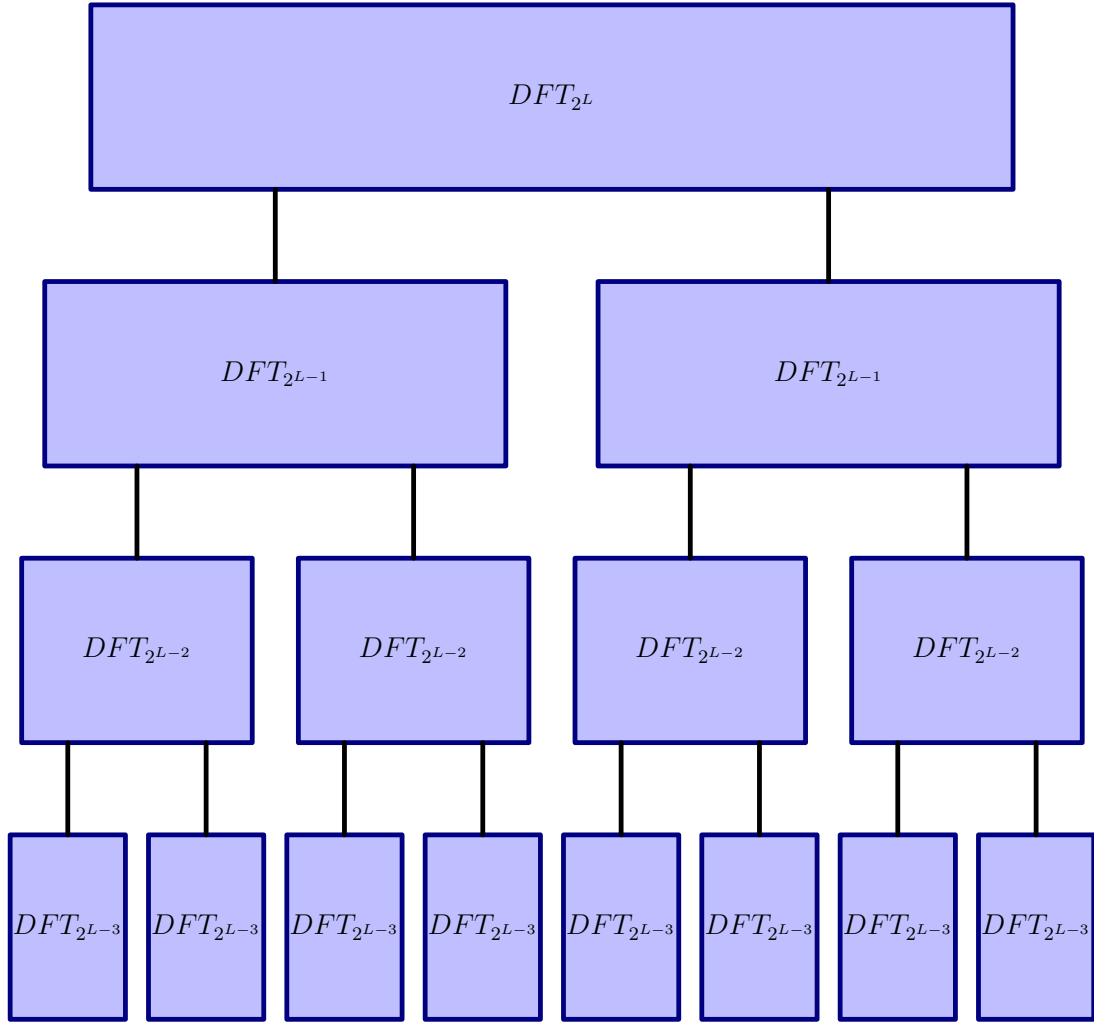
Figure 10: Recursive structure of the FFT algorithm for $N := 8$.

Lemma 4.5 (Complexity of the FFT). *The FFT algorithm has complexity $O(N \log N)$.*

Proof. For simplicity, we assume that $N = 2^L$ for some positive integer L; the argument can be adapted to the general case. The algorithm recursively decomposes the task of computing the DFT into a tree with L levels depicted in Figure 10. Let us number the levels starting at 0, which represents the root. At level $l \in \{1, \ldots, L\}$ there are 2^l nodes. At each node we need to compute Eq. (51), which amounts to scaling a vector of length 2^{L-l} and adding it to another vector of the same length. As a result at each level the complexity is of order $2^l 2^{L-l} = 2^L = N$. Since there are exactly $\log_2 N$ levels, the proof is complete. $\square$

Figure 11 shows a numerical comparison of the running time of the FFT and a naive matrix-based implementation of the DFT. The difference is dramatic, as expected from Lemma 4.5.

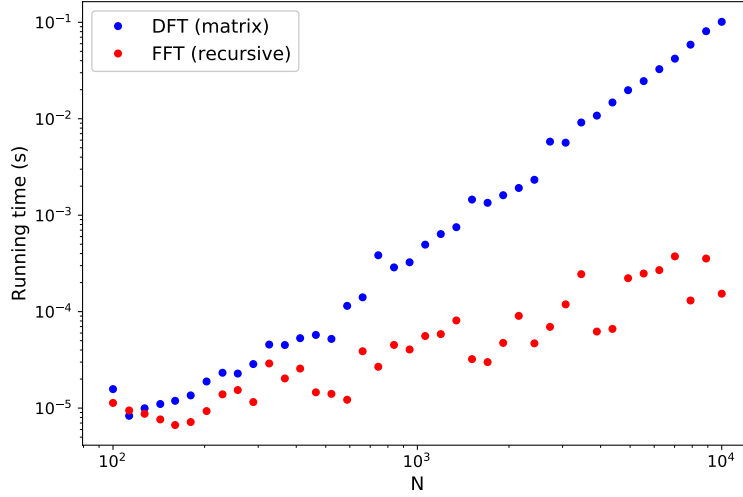Figure 11: Numerical comparison of the running times of a naive matrix-based implementation of the DFT (assuming the matrix is already built) and the FFT algorithm. Both approaches were applied to 20 random complex vectors for each value of N.

5 Fourier series of multidimensional signals

In this section we discuss the extension of frequency representations to multidimensional spaces. We consider the Hilbert space of complex-valued square-integrable functions defined on a hyper-rectangle $\mathcal{I} := [a_1, b_1] \times \ldots \times [a_p, b_p] \subset \mathbb{R}^p$ with the standard inner product,

$$\langle x, y \rangle := \int_{\mathcal{I}} x(t) \overline{y(t)} \, dt. \tag{52}$$

A natural multidimensional generalization of the sinusoid in Eq. (4) is

$$a \cos(2\pi \langle f, t \rangle + \theta). \tag{53}$$

Here the frequency f and the time variable t are d-dimensional vectors. The multidimensional sinusoid is periodic with period $1/\|f\|_2$ in the direction of the unit vector $\vec{v} := f/\|f\|_2$. Indeed,

$$a \cos\left(i2\pi \left\langle f, t + \frac{m}{\|f\|_2} \frac{f}{\|f\|_2} \right\rangle + \theta \right) = a \cos(i2\pi \langle f, t \rangle + i2\pi m + \theta) \tag{54}$$

$$= a \cos(i2\pi \langle f, t \rangle + \theta), \tag{55}$$

for any integer m. Multidimensional sinusoids are planar waves, constant along any hyperplane orthogonal to f. In the direction of f they oscillate with a frequency equal to the ℓ_2 norm of f. Figure 12 shows some examples. As in one dimension, working with complex sinusoids makes it easier to define frequency representations, because the phase can be encoded linearly as a complex multiplicative coefficient.

Definition 5.1 (Multidimensional complex sinusoids). *The complex sinusoid with frequency* $f \in R^d$ *is given by*

$$\exp(i2\pi \langle f, t \rangle) := \cos(2\pi \langle f, t \rangle) + i \sin(2\pi \langle f, t \rangle), \tag{56}$$

where $t \in \mathbb{R}^d$.

18

Any multidimensional sinusoid with frequency f can be expressed as the sum of two complex sinusoids with frequencies f and $-f$ respectively:

$$\cos\left(i2\pi\langle f, t\rangle + \theta\right) = \frac{\exp(i\theta)}{2}\exp(i2\pi\langle f, t\rangle) + \frac{\exp(-i\theta)}{2}\exp(-i2\pi\langle f, t\rangle). \tag{57}$$

Multidimensional complex sinusoids can be expressed as the product of complex sinusoids aligned with each axis.

$$\exp(i2\pi\langle f, t\rangle) := \exp\left(i2\pi\sum_{j=1}^{d} f[j]t[j]\right) \tag{58}$$

$$= \prod_{j=1}^{d}\exp(i2\pi f[j]t[j]). \tag{59}$$

For simplicity, and because we are mostly interested in applications related to images, from now on we focus on the two-dimensional case. However, most of the results generalize to higher dimensions. To alleviate notation, we denote each coordinate by $t_1 := t[1]$ and $t_2 := t[2]$. If turns out that for any fixed positive $T \in \mathbb{R}$, complex sinusoids with frequency coordinates equal to k_1/T and k_2/T for $k_1, k_2 \in \mathbb{Z}$ are all orthogonal. Figure 12 shows real-valued 2D sinusoids corresponding to different values of k_1 and k_2.

Lemma 5.2 (Orthogonality of multidimensional complex sinusoids). *The family of complex sinusoids with integer frequencies*

$$\phi_{k_1,k_2}^{2D}(t_1, t_2) := \exp\left(\frac{i2\pi k_1 t_1}{T}\right)\exp\left(\frac{i2\pi k_2 t_2}{T}\right), \qquad k_1, k_2 \in \mathbb{Z}, \tag{60}$$

is an orthogonal set of functions on any interval of the form $[a, a+T] \times [b, b+T]$, where $a, b, T \in \mathbb{R}$ and $T > 0$.

Proof. The result follows from Lemma 2.2. By Eq. (60)

$$\phi_{k_1,k_2}^{2D}(t_1, t_2) = \phi_{k_1}(t_1)\phi_{k_2}(t_2), \tag{61}$$

so that

$$\left\langle \phi_{k_1,k_2}^{2D}, \phi_{j_1,j_2}^{2D}\right\rangle = \int_{t_1=a}^{a+T}\int_{t_2=b}^{b+T} \phi_{k_1}(t_1)\phi_{k_2}(t_2)\overline{\phi_{j_1}(t_1)\phi_{j_2}(t_2)}\,\mathrm{d}t_1\,\mathrm{d}t_2 \tag{62}$$

$$= \langle\phi_{k_1}, \phi_{j_1}\rangle\langle\phi_{k_2}, \phi_{j_2}\rangle \tag{63}$$

$$= 0 \tag{64}$$

as long as $j_1 \neq k_1$ or $j_2 \neq k_2$. $\qquad\square$

The 2D Fourier series represents 2D functions in terms of complex sinusoids.
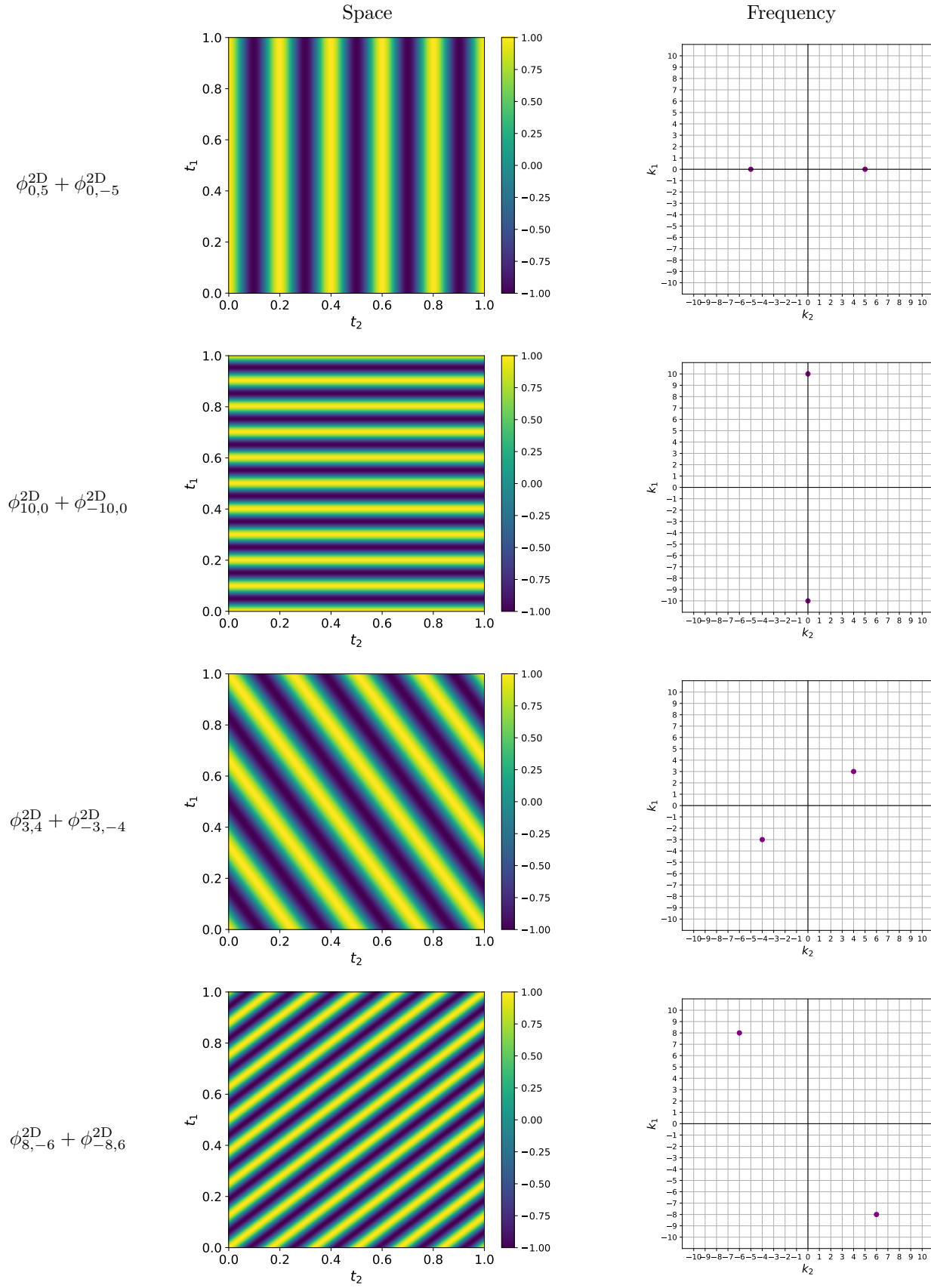
Figure 12: Spatial (left) and frequency (right) representation of real-valued 2D sinusoids with different 2D frequencies.
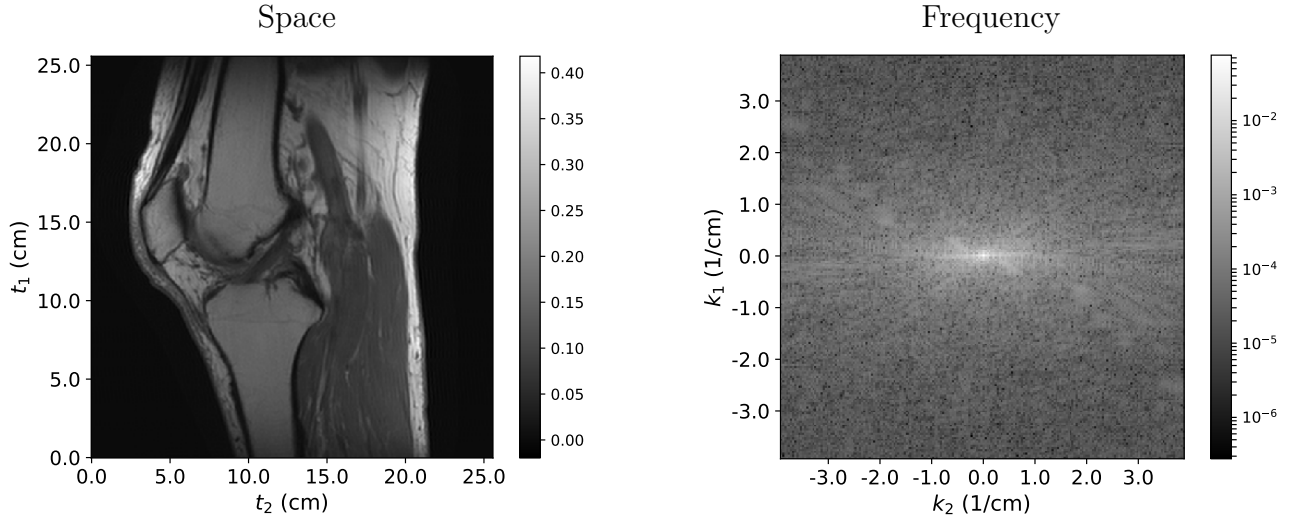
Figure 13: Sagittal section of a human knee measured by magnetic-resonance imaging. The image on the left shows the proton density of the section, whereas the image on the right shows the magnitude of the corresponding Fourier series coefficients.

Definition 5.3 (Fourier series). *The Fourier series coefficients of a function $x \in \mathcal{L}_2\left[a, a+T\right]$ for any $a, T \in \mathbb{R}$, $T > 0$, are given by*

$$\hat{x}[k_1, k_2] := \left\langle x, \phi^{2D}_{k_1, k_2} \right\rangle = \int_{t_1=a}^{a+T} \int_{t_2=b}^{b+T} x(t_1, t_2) \exp\left(-\frac{i2\pi k_1 t_1}{T}\right) \exp\left(-\frac{i2\pi k_2 t_2}{T}\right) \, dt_1 \, dt_2. \quad (65)$$

The Fourier series of order $k_{c,1}$, $k_{c,2}$ is defined as

$$\mathcal{F}_{k_{c,1}, k_{c,2}} \{x\} := \frac{1}{T} \sum_{k_1=-k_{c,1}}^{k_{c,1}} \sum_{k_2=-k_{c,2}}^{k_{c,2}} \hat{x}[k_1, k_2] \phi^{2D}_{k_1, k_2}. \quad (66)$$

As in the one-dimensional case, the Fourier series of a square-integrable function in multiple dimensions converges to the function as the order tends to infinity.

Example 5.4 (Magnetic resonance imaging). Magnetic resonance imaging (MRI) is a medical-imaging technique that measures the response of the atomic nuclei in biological tissues to high-frequency radio waves when placed in a strong magnetic field. Remarkably, the radio waves can be adjusted so that each measurement corresponds to a 2D Fourier coefficient of the proton density of the hydrogen atoms in a region of interest. In MRI the 2D frequency representation is called k-space. In order to reconstruct an MRI image, we compute the Fourier series corresponding to the k-space measurements. Figure 13 shows an example. In this case, $T := 25$ cm, so that the basic frequency in the Fourier series equals 0.04 cm^{-1}. Figure 14 shows the Fourier series for different values of $k_{c,1}$ and $k_{c,2}$. These values govern the vertical and horizontal resolution of the image. $\triangle$
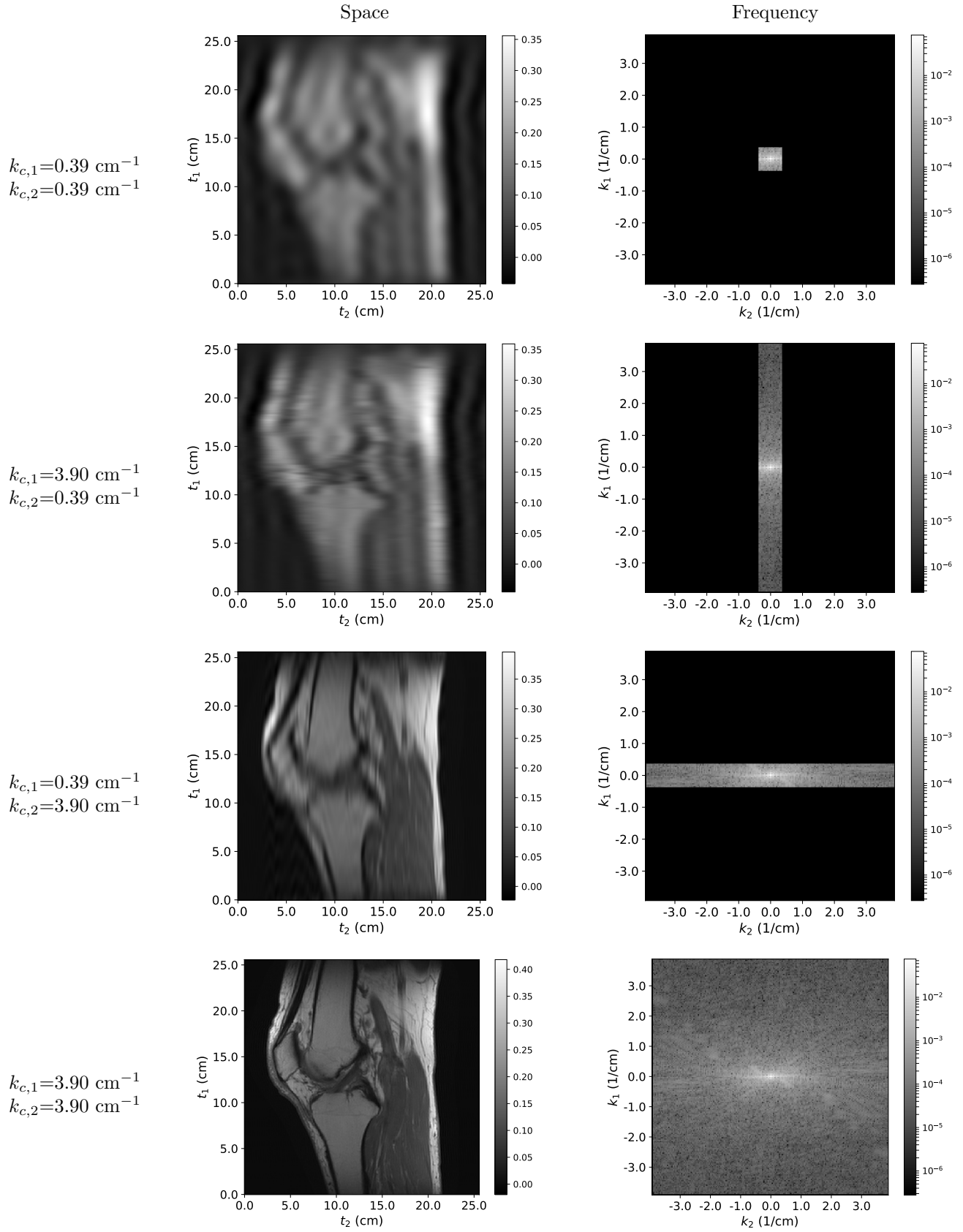
Figure 14: On the right, Fourier series of the image in Figure 13 for different values of $k_{c,1}$ and $k_{c,2}$. The magnitude of the corresponding Fourier coefficients is shown on the right.

6 Sampling theorem in 2D

As in one dimension, bandlimited signals are signals that are well represented by a finite number of Fourier-series coefficient, like the image in Figure 13. To simplify the definition, we consider Fourier series that have the same order in the vertical and horizontal indices.

Definition 6.1 (Bandlimited signal). *A signal defined on the 2D rectangle $[a, a + T] \times [b, b + T]$, where $a, b, T \in \mathbb{R}$ and $T > 0$ is bandlimited with a cut-off frequency k_c if it is equal to its Fourier series representation of order k_c, i.e.*

$$x(t_1, t_2) = \sum_{k_1=-k_c}^{k_c} \sum_{k_2=-k_c}^{k_c} \hat{x}[k_1, k_2] \exp\left(\frac{i2\pi k_1 t_1}{T}\right) \exp\left(\frac{i2\pi k_2 t_2}{T}\right). \tag{67}$$

Bandlimited functions can be exactly recovered from a finite number of samples. To simplify notation we consider functions supported on the square $[0, T)^2$ for some real $T > 0$, without loss of generality. We will focus on equispaced sampling patterns of the form:

$$X_{[N]} := \begin{bmatrix} x\left(\frac{0}{N}, \frac{0}{N}\right) & x\left(\frac{0}{N}, \frac{T}{N}\right) & \cdots & x\left(\frac{0}{N}, T - \frac{T}{N}\right) \\ x\left(\frac{T}{N}, \frac{0}{N}\right) & x\left(\frac{T}{N}, \frac{T}{N}\right) & \cdots & x\left(\frac{T}{N}, T - \frac{T}{N}\right) \\ \cdots & \cdots & \cdots & \cdots \\ x\left(T - \frac{T}{N}, \frac{0}{N}\right) & x\left(T - \frac{T}{N}, \frac{T}{N}\right) & \cdots & x\left(T - \frac{T}{N}, T - \frac{T}{N}\right) \end{bmatrix}. \tag{68}$$

The sampling theorem, generalized to 2D, provides a condition on N to ensure exact recovery of the bandlimited signal from such measurements.

Theorem 6.2 (Nyquist-Shannon-Kotelnikov sampling theorem). *Any bandlimited signal $x \in \mathcal{L}_2[0, T)^2$, where $T > 0$, with cut-off frequency k_c can be recovered exactly from N^2 uniformly spaced samples as long as*

$$N \geq 2k_c + 1, \tag{69}$$

where $2k_c + 1$ is known as the Nyquist rate. *Recovery can be carried out by obtaining the matrix of Fourier series coefficients*

$$\widehat{X}_{[k_c]} := \begin{bmatrix} \hat{x}_{-k_c,-k_c} & \hat{x}_{-k_c,-k_c+1} & \cdots & \hat{x}_{-k_c,k_c} \\ \hat{x}_{-k_c+1,-k_c} & \hat{x}_{-k_c+1,-k_c+1} & \cdots & \hat{x}_{-k_c+1,k_c} \\ \cdots & \cdots & \cdots & \cdots \\ \hat{x}_{k_c,-k_c} & \hat{x}_{k_c,-k_c+1} & \cdots & \hat{x}_{k_c,k_c} \end{bmatrix} \tag{70}$$

from the vector of samples $X_{[N]}$ as follows

$$\widehat{X}_{[k_c]} = \frac{1}{N^2} \widetilde{F}^*_{[N]} X_{[N]} \left(\widetilde{F}^*_{[N]}\right)^T, \tag{71}$$

where $\widetilde{F}_{[N]}$ is defined in Eq. (32).

Proof. The result follows from the identity

$$X_{[N]} = \widetilde{F}_{[N]} \widehat{X}_{[k_c]} \widetilde{F}_{[N]}^T, \tag{72}$$

which can be verified by computing the matrix product, and from the fact that $\frac{1}{\sqrt{N}} \widetilde{F}_{[N]}$ is an orthogonal matrix by Lemma 7.2. $\qquad\square$

7   Discrete Fourier transform in 2D

In this section we extend the definition of discrete Fourier transform to two dimensions. We represent discrete signals in 2D as matrices belonging to the vector space of $\mathbb{C}^{N \times N}$ matrices endowed with the standard inner product

$$\langle A, B \rangle := \operatorname{tr} (B^* A), \quad A, B \in \mathbb{C}^{N \times N}. \tag{73}$$

This is equivalent to representing the signals as vectors in $\mathbb{C}^{N^2}$ with the usual dot product. Discrete complex sinusoids form a basis of the space.

Definition 7.1 (Discrete complex sinusoids)**.** *The discrete complex sinusoid $\psi_{k_1,k_2}^{\mathrm{2D}} \in \mathbb{C}^{N \times N}$ with integer frequencies k_1 and k_2 is defined as*

$$\psi_{k_1,k_2}^{\mathrm{2D}}[j_1, j_2] := \exp \left(\frac{i 2 \pi k_1 j_1}{N} \right) \exp \left(\frac{i 2 \pi k_2 j_2}{N} \right), \qquad 0 \le j_1, j_2 \le N - 1, \tag{74}$$

or, in terms of 1D discrete sinusoids

$$\psi_{k_1,k_2}^{\mathrm{2D}} = \psi_{k_1} \psi_{k_2}^T. \tag{75}$$

Lemma 7.2 (Orthonormal sinusoidal basis)**.** *The discrete complex exponentials $\frac{1}{N} \psi_{k_1,k_2}^{\mathrm{2D}}$, $0 \le k_1, k_2 \le N - 1$, form an orthonormal basis of $\mathbb{C}^{N \times N}$.*

Proof. By Eq. (76), we can reformulate the inner product of two 2D discrete sinusoids in terms of 1D discrete sinusoids

$$\langle \psi_{k_1,k_2}^{\mathrm{2D}}, \psi_{l_1,l_2}^{\mathrm{2D}} \rangle = \operatorname{tr} \left(\left(\psi_{l_1,l_2}^{\mathrm{2D}} \right)^* \psi_{k_1,k_2}^{\mathrm{2D}} \right) \tag{76}$$

$$= (\psi_{k_1})^* \psi_{l_1} (\psi_{k_2})^* \psi_{l_2}. \tag{77}$$

Lemma 7.2 then implies that the inner product equals N if $k_1 = l_1$ and $k_2 = l_2$, and zero otherwise. Since there are N^2 vectors in the set and they are linearly independent, they form a basis of $\mathbb{C}^{N^2}$. $\qquad\square$

The 2D discrete Fourier transform is just a change of basis that expresses a 2D vector in terms of 2D discrete complex sinusoids.

Definition 7.3 (2D discrete Fourier transform). *The discrete Fourier transform (DFT) of a 2D array $X \in \mathbb{C}^{N \times N}$ is given by*

$$\widehat{X}[k_1, k_2] := \left\langle X, \psi_{k_1,k_2}^{2\mathrm{D}} \right\rangle, \qquad 0 \leq k_1, k_2 \leq N - 1, \tag{78}$$

or equivalently by

$$\widehat{X} := F_{[N]} X \, F_{[N]}, \tag{79}$$

where $F_{[N]}$ is the 1D DFT matrix defined in Eq. (46). The inverse DFT of a 2D array $\widehat{Y} \in \mathbb{C}^{N \times N}$ equals

$$Y = \frac{1}{N^2} F_{[N]}^* \widehat{Y} \, F_{[N]}^*. \tag{80}$$

Recall that by Lemma 7.2 the rows (and columns) of $F_{[N]}$ are orthogonal and have norm $\sqrt{N}$, which justifies the definition of the inverse DFT.

Corollary 7.4. *The inverse 2D DFT inverts the 2D DFT.*

As in one dimension, if we interpret the entries of a matrix X as equispaced samples from a bandlimited signal measured at the Nyquist rate, then the 2D DFT of X is exactly equal to the 2D Fourier series of x (recall that the rows of $F_{[N]}$ are the same as the rows of $\widetilde{F}_{[N]}$, only in a different order). By Lemma (4.5), the complexity of computing the 2D DFT using the FFT algorithm is $O(N^2 \log N)$. In contrast, a naive implementation using matrix-vector multiplications would have complexity $O(N^3)$.